AN EXACT CALCULATION METHOD OF NONLINEAR OPTIMAL CONTROLS AND APPLICATIONS IN AEROSPACE FIELDS

FUMIAKI IMADO
Department of Mechanical Systems Engineering
Shinshu University
4-17-1 Wakasato Nagano, Nagano 380-8553
JAPAN
http://www.shinshu-u.ac.jp

Abstract: Obtaining optimal controls for high-dimensional nonlinear dynamic systems is very important, but generally very difficult. Authors have developed some solvers based on classical gradient methods, which can automatically obtain the converged solutions by introducing a lot of expertise based on our former experiences. This paper shows some examples of nonlinear optimal control problems in aerospace fields and their solutions obtained by our program. Some key technologies introduced into the program are briefly explained. The program is also useful to solve differential game problems, and an application is also shown.

Keywords: - Nonlinear Optimal Controls, Differential Games, Satellites, Missiles, Aircraft, STP-CODE

1 Introduction

Obtaining optimal controls for high-dimensional nonlinear dynamic systems is very important, but generally very difficult. Until the 1980s several regular methods such as the steepest gradient method had been developed and employed. After that, direct shooting methods with mathematical programming, or Neural nets became very popular, and their presence on the market has made the regular methods obsolete. These new methods are easy to use even for beginners. However, they can obtain only approximate solutions without precision. Also, they cannot apply to high-dimensional complicate problems. The main reason why the old regular methods are obsolete is, they require the user's experience and expertise to converge solutions. Authors have developed some solvers which are based on the classical steepest ascent method [1], the Successive Conjugate Gradient Restoration Algorithm (SCGRA) [2] etc. These solvers can automatically obtain the converged solutions by introducing a lot of expertise based on our former experiences. Among them, the algorithm of one solver, the STP-CODE is employed to solve these example problems. In this paper, the required formulation for the STP-CODE is explained first. For readers' convenience, the details of the algorithm are shown in the Appendix. In section 3, satellite orbit transfer problems with low thrusts are explained. In section 4, missile-aircraft pursuit-evasion problems are explained. The one-sided optimal control problem is extended to two-sided optimal control problems (differential games) in section 5. Some key technologies of the STP-CODE are explained in section 6.

2 Problem Formulation

In order to employ the STP-CODE (STeePest ascent CODE), the problems must be defined as follows.

Find $\bar{u}(t)$ to maximize (for minimizing, change the sign of the following ϕ)

$$J = \phi[\bar{x}(t_f)] \tag{1}$$

where

$$\dot{\bar{x}} = \bar{f}(\bar{x}, \bar{u}, t) \tag{2}$$

$$\bar{x}(t_0) = \bar{x}_0 \quad : \text{specified} \tag{3}$$

with terminal constraints

$$\bar{\psi}[\bar{x}(t_f), t_f] = 0 \tag{4}$$

where $\bar{x}(t)$ is an n-dimensional state vector, $\bar{u}(t)$ is an m-dimensional control vector, and $\bar{\psi}$ is a q-dimensional constraint vector. The terminal time t_f is determined from the following stopping condition:

$$\Omega[\bar{x}(t_f), t_f] = 0 \tag{5}$$

In (5), Ω can be selected from one arbitrary component of $\bar{\psi}$ in (4), however, it must clearly determine the final time t_f. Generally, it is easier to inflict the constraints (4) by introducing penalty functions rather than following the method in the Appendix of this paper. As for this point, an explanation is added in section 6.

3 Optimal Orbit Transfer of a Satellite with Low Thrusts

Fig.1 shows the inertial coordinates and symbols. Fig.2 shows the satellite orbit coordinates and symbols. The equations of motion are given as follows [3],[4].

$$\dot{x} = v_x \quad \dot{y} = v_y \quad \dot{z} = v_z$$

$$\dot{v}_x = -\frac{\mu}{r^3}\left\{1-\frac{3r_e^2}{r^2}J_2\left(\frac{5}{2}\frac{z^2}{r^2}-\frac{1}{2}\right)\right\}x + f_x + d_x$$

$$\dot{v}_y = -\frac{\mu}{r^3}\left\{1-\frac{3r_e^2}{r^2}J_2\left(\frac{5}{2}\frac{z^2}{r^2}-\frac{1}{2}\right)\right\}y + f_y + d_y$$

$$\dot{v}_z = -\frac{\mu}{r^3}\left\{1-\frac{3r_e^2}{r^2}J_2\left(\frac{5}{2}\frac{z^2}{r^2}-\frac{1}{2}\right)\right\}z + f_z + d_z \quad (6)$$

$$\dot{m} = -k(|f_{x0}|+|f_{y0}|+|f_{z0}|) \quad (7)$$

where

μ: gravity constant 398600.9 (km^3/s^2)

r_e: mean earth equatorial radius 6378.143 km

J_2: zonal second coefficient 1082.628E-6

f_x, f_y and f_z are control force components, d_x, d_y, and d_z are drag force components, and k is the fuel consumption coefficient, f_{x0}, f_{y0}, and f_{z0} are the thrust components of the satellite fixed thrusters per unit mass. By the transformation of coordinates shown in Figs 1 and 2, the following relations exist.

$$\begin{aligned} f_x &= (-c\Omega s\eta - s\Omega cic\eta) f_{x0} + (-s\Omega si) f_{y0} \\ &\quad +(-c\Omega c\eta + s\Omega cis\eta) f_{z0} \\ f_y &= (-s\Omega s\eta + c\Omega cic\eta) f_{x0} + (c\Omega si) f_{y0} \\ &\quad +(-s\Omega c\eta - c\Omega cis\eta) f_{z0} \\ f_z &= (sic\eta) f_{x0} + (-ci) f_{y0} + (-sis\eta) f_{z0} \end{aligned} \quad (8)$$

In vector notation, the above variables are expressed as,

$$\bar{x} = (x, y, z, v_x, v_y, v_z, m)^T \quad (9)$$

$$\bar{u} = (f_{x0}, f_{y0}, f_{z0})^T \quad (10)$$

A general optimal orbit transfer problem is defined as finding the optimal control histories $\bar{u}$ under the above equations to maximize the next performance index ϕ ,

$$\phi = \left\{m - (\bar{\psi} - \bar{\psi}_f)^T K (\bar{\psi} - \bar{\psi}_f)\right\}_{t=t_f} \quad (11)$$

where the elements of the terminal constraint vector $\bar{\psi}$ are arbitrary functions of states, K is an arbitrary penalty coefficient matrix, and t_f is the final time. The following constraints are also imposed on control variables.

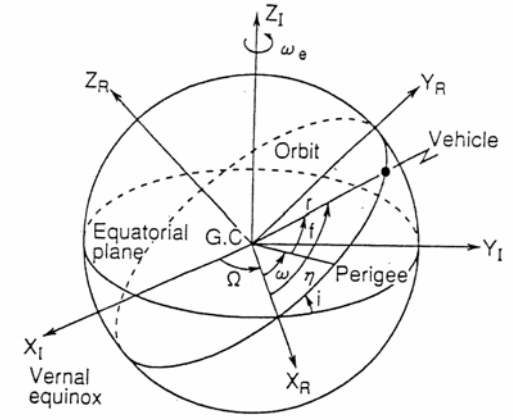

Fig.1 Inertial coordinates and symbols

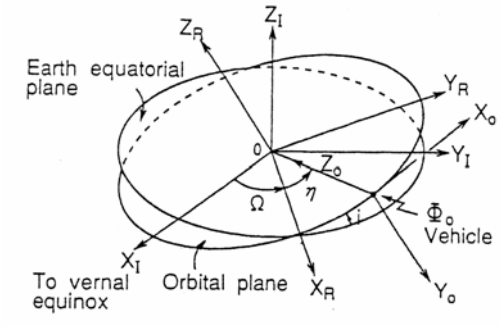

Fig.2 Orbit coordinates and symbols

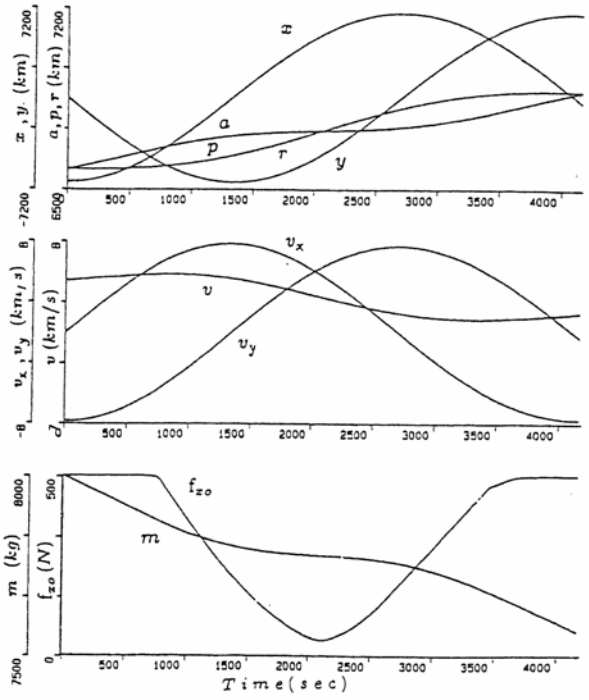

Fig.3 Orbit variables' histories (coplanar orbit)

$$-f_{\max} \le f_{x0}(t) \le f_{\max}$$
$$-f_{\max} \le f_{y0}(t) \le f_{\max}$$
$$-f_{\max} \le f_{z0}(t) \le f_{\max} \quad (12)$$

In order to apply the STP-CODE, the partial derivatives of the right side of Eqs. (6),(7) by $\bar{x}$ and $\bar{u}$ are required. Although the orbital parameters Ω, η, i etc. are expressed as the functions of these variables, these derivatives are obtained, but the explicit expressions are too complicated and are abbreviated here. Some calculation results are explained as follows.

Optimal orbit transfer from a 200km altitude to a 500km altitude circular orbit with fixed thrusters of 500N thrust is calculated. Fig.3 shows some orbit parameters' histories, where a and p are the orbit semimajor axis and semilatus rectum, respectively. The initial mass of the vehicle is 8000kg. the performance index and terminal constraints in this problem are given as follows,

$$\phi = m_f - kt_f \quad (13)$$
$$\overline{\psi} = (a - a_f, p - p_f)^T_{t_f} = (0,0)^T_{t_f} \quad (14)$$

Eq. (13) means maximizing final mass (minimizing the fuel consumption) within less time (the priority is the fuel) . Only f_{x0} is employed here, and the fuel consumption is only 2.4% larger than the ideal Hohman transfer where the thrust magnitude is infinity. Figs 4 – 6 show the case where the orbit inclination is changed from 30deg. to 35deg. In this case, the following constraint is applied instead of (14),

$$\overline{\psi} = (a - a_f, p - p_f, i - i_f)^T_{t_f} = (0,0,0)^T_{t_f} \quad (15)$$

The results of Figs 4 and 5 produce the same fuel consumption, therefore these are both the solution of this optimal control problem. On the other hand, the solution in Fig. 6 requires larger fuel consumption, therefore this is only a local optimum solution. Although the gradient methods are said to be not efficient for bang-bang type solutions, however, very crisp bang-bang type controls are obtained by the STP-CODE

4 Fighter Evasive Maneuvers Against Proportional Navigation Missile

Perhaps this problem had been solved by authors and published for the first time in Aug.1983 as AIAA paper-83-2139. The results with some extended studies were published in 1986 [5]. Since then, the problem has attracted many researchers' interests and a large amount of studies have been conducted until now. Fig. 7 shows the relative geometry of the pursuer and the evader and symbols. Here, the pursuer is a missile, and the evader is an aircraft. Both vehicles are modeled as point masses, and the equations of motion in a horizontal plane are as follows.

$$\dot{v}_t = (T_t \cos\alpha - D)/m_t \quad (16)$$
$$\dot{\psi}_t = (L + T_t \sin\alpha)/(m_t v_t) \quad (17)$$
$$\dot{x}_t = v_t \cos\psi_t \quad (18) \qquad \dot{y}_t = v_t \sin\psi_t \quad (19)$$
$$L = (1/2)\rho_t {v_t}^2 S_t C_L \quad D = (1/2)\rho_t {v_t}^2 S_t C_D \quad (20)$$
$$C_L = C_{L\alpha}(\alpha - \alpha_0) \quad C_D = C_{D0} + k{C_L}^2 \quad (21)$$

A constraint is imposed on the value of the aircraft lateral acceleration a_t, which is treated as the

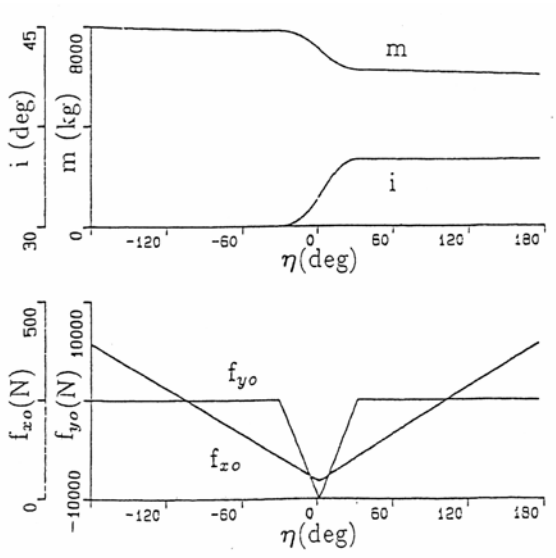

Fig.4 Mass, inclination, and control histories ($f_{\max}$ =10,000N, =35deg., type 1)

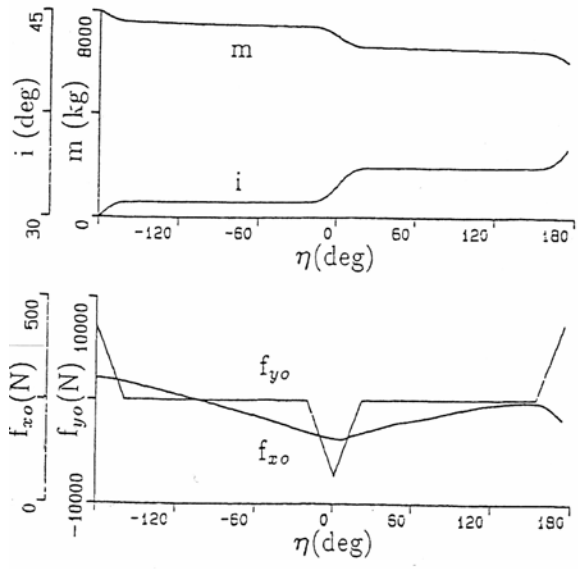

Fig.5 Mass, inclination, and control histories ($f_{\max}$ =10,000N, =35deg., type 2)

aircraft control variable. $a_t = L/m_t \le a_{t\max}$ (22)
The missile lateral acceleration is approximated by a first-order lag to a lateral acceleration command a_{mc}, which is treated as the missile control variable. The missile equations of motion are given by,

$$\dot{v}_m = 1/m_m(T_m - D_m) \quad (23) \qquad \dot{a}_m = (a_{mc} - a_m)/\tau \quad (24)$$
$$\dot{\psi}_m = a_m / v_m \quad (25) \qquad \dot{x}_m = v_m \cos\psi_m \quad (26)$$
$$\dot{y}_m = v_m \sin\psi_m \quad (27)$$

where

$$D_m = k_1 v_m^2 + k_2 (a_m / v_m)^2 \quad (28)$$
$$k_1 = (1/2)\rho_m S_m C_{D0m} \quad k_2 = 2k_m m_m^2/(\rho_m S_m) \quad (29)$$

where

$$T_m(t) = \begin{cases} T_m & for \quad 0 < t \le t_e \\ 0 & for \quad t_e < t \end{cases} \quad (30)$$

For the PNG missile with signal saturation taken into consideration, a_{mc} is given by

$$a_{mc} = \begin{cases} N_e v_c \dot{\sigma} & for \quad |a_{mc}| \le a_{mc\max} \\ a_{mc\max} sign(a_c) & for \quad |a_{mc}| > a_{mc\max} \end{cases} \quad (31)$$

In Eq.(31), N_e is the effective navigation ratio, v_c the closing velocity, and $\dot{\sigma}$ the line-of-sight turning rate given by

$$v_c = -\dot{r} \quad (32)$$
$$\dot{\sigma} = 1/r^2 [(y_t - y_m)(\dot{x}_t - \dot{x}_m) \quad (33)$$

where r is slant range,

$$r = \left[(x_t - x_m)^2 + (y_t - y_m)^2\right]^{1/2} \quad (34)$$

Our purpose is to obtain the optimal control histories of the aircraft that maximize the final MD (Miss Distance) which is the slant range at the CAP (Closest Approach Point). Therefore, the performance index ϕ and the stopping condition Ω is given by,

$$\Omega \equiv v_c = 0 \quad (35), \quad \phi = (r)_{t_f} \quad (36)$$

Typical parameters of the vehicles in our studies are,

Aircraft (afterburner)

$m_t = 7500kg \quad h_{t0} = 4572m \quad S_t = 26m^2$
$v_{t0} = 290.2m/s \ (0.9M) \quad C_{L\alpha} = 3.689/rad$
$C_{D0} = 0.0224 \quad k = 0.260 \quad a_{t\max} = 9g$
Engine : PWF-100 $T_{\max} = T_{\max}(v, h)$

Missile (Sustainer phase)

$m_{m0} = 173.6kg \quad I_{SP} = 250s \quad T_m = 6000N$
$t_e = 8s \quad S_m = 0.0324m^2 \quad h_{m0} = 4572m$
$v_{m0} = 644.6m/s \ (2.0M) \quad C_{L\alpha} = 35.0/rad$
$C_{D0} = 0.90 \quad k = 0.030 \quad a_{c\max} = 30g$
$\tau = 0.5s \quad Ne = 4.0$

Typical vehicle trajectories and aircraft control histories are shown in Fig. 8.
This missile avoidance problem and derivation can be extended to multiple missile cases. For the purpose, the authors introduced a penalty function with a window function [6] as follows.

$$\dot{p} = w(t)(r_{lt}/r_1)^n \quad (37)$$
$$w(t) = \begin{cases} 1.0 \ for \ t_{w1} \le t \le t_{w2} \\ 0 \ for \ 0 \le t < t_{w1}, t_{w2} < t \end{cases} \quad (38)$$

where t_{w1} and t_{w2} are selected to include the time of CAP against the first missile between them. The following performance index is selected.

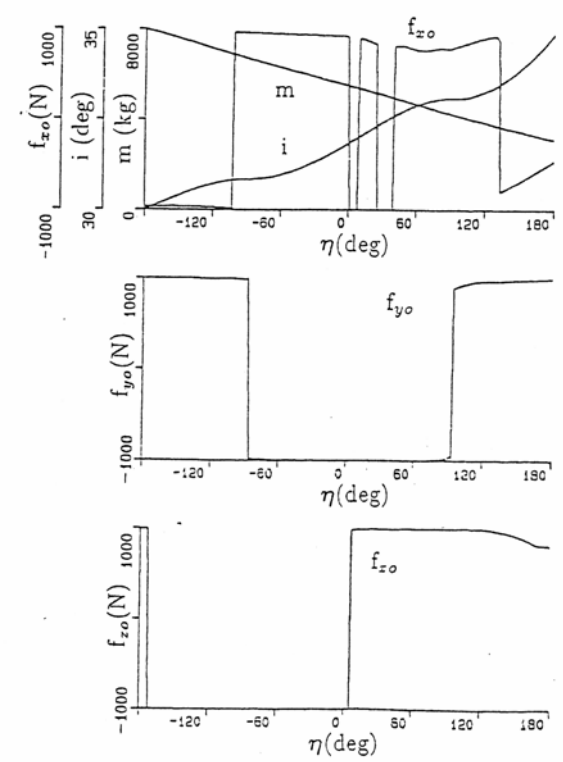

Fig.6 Mass, inclination, and control histories
($f_{\max}$ =10,000N, =35deg., type 3)

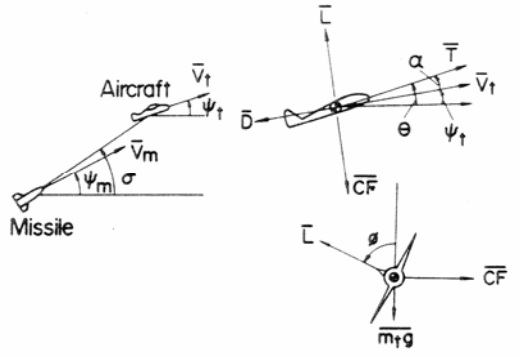

Fig.7 Vehicle geometry and symbols

$$\phi = \{k_r r_2^{\,2} - k_{rf}(r_2 - r_{2f})^2 - k_p p\}_{tf} \quad (39)$$

where the terminal time t_f is obtained from the following stopping condition

$$\Omega = \dot{r}_2 = 0 \quad (40)$$

which means the time of the CAP with the second missile. As the penalty $k_p p$ in (39) tries to maximize the MD between the first missile and the aircraft, therefore by selecting the coefficients in (39) appropriately, we can make both MDs between two missiles as large as possible. Note that by the above method, we can reduce a multi-point boundary value problem to a two-point boundary value problem.

5 Pursuit-Evasion Problems of Two Cars in an Ellipsoid Under Gravity.

The STP-CODE is also useful to solve differential game problems. In former studies, the author has shown two methods to solve practical nonlinear differential game problems by employing one-sided nonlinear optimal control solvers.

(1) Start from a nominal solution, where the pursuer (missile) is guided by PNG (Proportional Navigation Guidance: a kind of quasi-optimal control), while the evasive target (fighter) takes one-sided non-linear optimal control. The solution is iteratively corrected to converge into a mini-max solution. One successful result is shown in [7].

(2) Both players take their one-sided optimal controls, and find the tangent point of their reachable terminal surfaces. One successful result is shown in [8].

In [7] and [8], missile-aircraft pursuit-evasion differential games are solved. Here, the author's recent study, pursuit-evasion problems of two cars in an ellipsoid are briefly explained. In solving these problems, the second method above is employed.

Fig.9 shows a car in an ellipsoid and some symbols. The equation of the ellipsoid is given by

$$R(x,y,z) \equiv \frac{x^2}{d^2} + \frac{y^2}{e^2} + \frac{z^2}{f^2} - 1 = 0 \quad (41)$$

By introducing subsidiary parameters u, v

$$x = d\cos u\cos v \quad y = e\cos u sinv \quad z = f\, sinu \quad (42)$$

The coordinates of p in the plane are expressed by employing u, and v

$$p(u,v) = (x(u,v), y(u,v), z(u,v)) \quad (43)$$

The tangential lines of u and v directions at p are given by

$$p_u = \partial p / \partial u = (x_u, y_u, z_u)$$

$$p_v = \partial p / \partial v = (x_v, y_v, z_v) \quad (44)$$

The normal vector at p is given by ν, where

$$\nu = \frac{p_u \times p_v}{|\, p_u \times p_v \,|} \quad (45)$$

Fig.10 shows the force balance and control variables of the car a and ψ, where a and F_g are the acceleration and gravity force components parallel to the surface. The following constraints are imposed on controls.

$$0 \le a \le a_{\max} \quad , \quad -\pi \le \psi \le \pi \quad (46)$$

The rotation matrix around the vector ν is given by

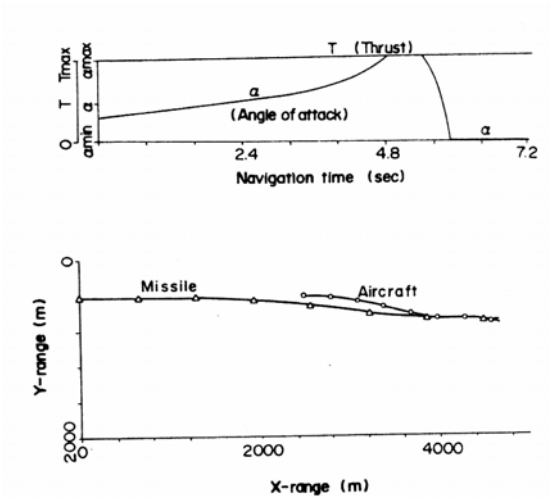

Fig.8 A typical aircraft optimal evasive maneuver (tail chase)

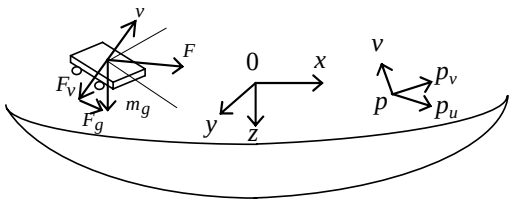

Fig.9 A car in an ellipsoid

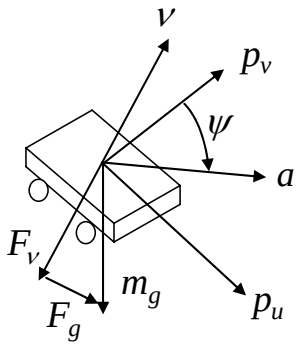

Fig.10 Control variables

$$\begin{bmatrix} v_x^2 V_\psi + c\psi & v_x v_y V_\psi - v_x s\psi & v_x v_z V_\psi + v_y s\psi \\ v_x v_y V_\psi + v_z s\psi & v_x^2 V_\psi + c\psi & v_y v_z V_\psi - v_x s\psi \\ v_x v_z V_\psi - v_y s\psi & v_y v_z V_\psi + v_x s\psi & v_z^2 V_\psi + c\psi \end{bmatrix} \quad (47)$$

where V_ψ is $1 - c\psi$

By differentiating (42) two times and with some manipulations, we obtain

$$\ddot{u} = -(c_1 ecv + c_2 dsv)/(desu) \qquad su \neq 0$$
$$\ddot{v} = -(c_1 esv - c_2 dcv)/(decu) \qquad cu \neq 0 \quad (48)$$

where

$$c_1 = a_x + g_x + d_x + d[(\dot{u}^2 + \dot{v}^2)cucv - 2\dot{u}\dot{v}susv)]$$
$$c_2 = a_y + g_y + d_y + e[(\dot{u}^2 + \dot{v}^2)cusv + 2\dot{u}\dot{v}sucv)] \quad (49)$$

where a_x and a_y are x and y components of a obtained through rotation matrix (47). g_x, g_y and d_x, d_y are acceleration (deceleration) caused by gravity and drag, respectively. By expressing as

$$\dot{u} = V_u \quad , \quad \dot{v} = V_v \quad (50)$$

the equations of motion of the car are expressed by four-dimensional first order simultaneous differential equations, and can be supplied to the STP-CODE. Above equations are applied to both evader and pursuer.

Fig.11 shows a calculation example where an ellipsoid of d =3000m, e =1500m, and f =300m is selected. The initial position, velocity of P and E are x_{p0} = 0m, y_{p0} =-100m, V_{p0}=15m/s, x_{e0}= 0m, y_{e0}=-250m, V_{e0}=5m/s, and their accelerations (naturally they always employ their maximum values) are $a_{p\max} = 2m/s^2$ and $a_{e\max} = 1.5m/s^2$, respectively. The initial offset angle of P is 15degrees from Y axis. Given an arbitrary time T, both players try to run as far as possible, and their reachable terminal surfaces for T=11s to 17s are shown. Clearly, the mini-max solution occurs at T=17s where the terminal surfaces produce a tangent point. Fig.12 shows the evader's optimal trajectory and the pursuer's nominal and optimal trajectories (a set of nominal control histories is required before starting iterations by the STP-CODE) . Fig.13 shows the pursuer's nominal and optimal control histories. The difference of the capture time of the optimal and nominal controls is at most 20ms, which is about 0.01% of the total time. That is, the sensitivity of the controls to the performance index is very small, therefore, by a recent easy method, it will be difficult to obtain this solution.

Necessary conditions of the solution

As the common performance index is the capture time, the system Hamiltonian becomes as

$$H = 1 + \lambda^T f \quad (50) \quad \text{where} \quad f = (\dot{u}, \dot{v}, \dot{V}_u, \dot{V}_v)^T \quad (51)$$

and λ is the adjoint vector.

The control vectors of both pursuer and evader are,

$$u_p = (\psi_p, a_p)^T \quad \text{and} \quad u_e = (\psi_e, a_e)^T \quad (52)$$

The necessary (stationary) conditions for the mini-max solution are as follows.

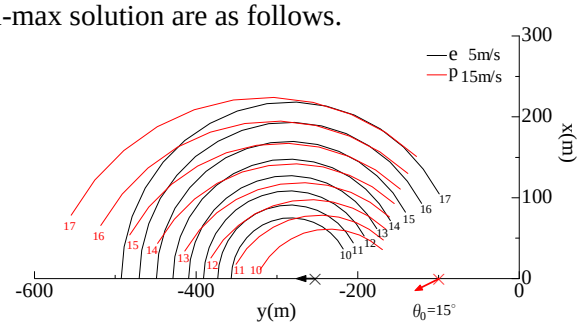

Fig.11 Offset angle=15deg. without drag.

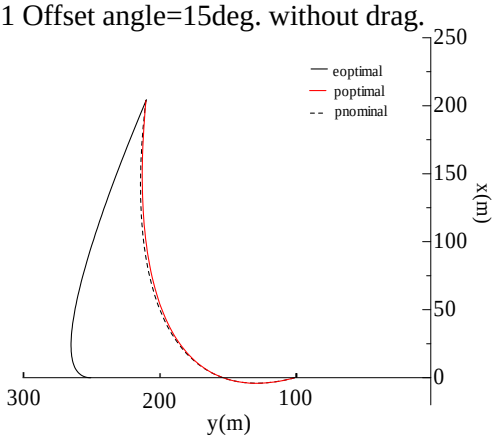

Fig.12 Optimal and nominal trajectories of vehicles

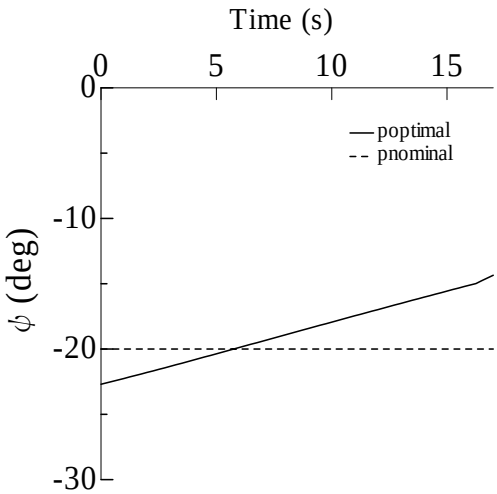

Fig.13 Nominal and optimal controls of the pursuer

$$\frac{\partial H}{\partial \psi_p} = 0 \ , \quad a_p = a_{p\max}$$
$$\frac{\partial H}{\partial \psi_e} = 0 \ , \quad a_e = a_{e\max}$$
$$for \ \ 0 \le t \le t_f \qquad (53)$$

As for symbols employed in above equations, see the appendix. The above characteristics are automatically satisfied by the nature of the steepest ascent algorithm. The saddle point condition (Nash Equilibrium) is satisfied in the result.

$$J\left[u_p^0(t), u_e(t)\right] < J\left[u_p^0(t), u_e^0(t)\right] < J\left[u_p(t), u_e^0(t)\right]$$
$$for \quad 0 \le t \le t_f \qquad (54)$$

where $u_p^0(t)$ and $u_e^0(t)$ are optimal solutions of u_p and u_e, respectively. The above characteristics are assured by the proposed algorithm. It is also verified by contradiction. That is, by selecting arbitrary differential changes from the optimal control of one vehicle and calculating corresponding one-sided optimal control of the opponent vehicle and conducting simulations.

6 Some Techniques for Automatic Convergence in STP-CODE

There are a lot of expertise and experiences introduced in the STP-CODE. Some of the techniques are explained here.

At first, some facts known to us by former experiences are stated.

(1) The characteristics of convergence (COC) do not depend on the number of states, and complexity of systems. COC depends on the number of controls and time steps. With up to three controls and up to 200 time steps, we usually could obtain the solution easily, but if the numbers increase farther, COC severely degrades.

(2) It is easier to introduce constraints to the performance index by penalty functions, than to treat them by the formal method written in the Appendix. In order to simultaneously select appropriate penalty coefficients, a special technique is employed, which is explained later.

The key techniques of the steepest ascent algorithm is the proper choice of the value *dp* which appeares in (A-22), which must be changed every step, and how to avoid dropping into local optima, and to reach the global optimum. Some features of the STP-CODE are,

(1) The program is written in FORTRAN.

(2) Not only is the suitable *dp* automatically selected, but also the convergence procedure is accelerated.

(3) An algorithm is introduced to automatically avoid dropping into local optima, and to reach the global optimum.

(4) In order to satisfy constraints by penalty functions, very large values must be selected, however, this often causes the solution to drop into local optima and further iteration is stopped. In the case, the constraints are relaxed and the penalty coefficients are decreased. After the iteration is recovered, then the penalty coefficients are gradually increased again.

The processes (3) and (4) can not be implemented by only the FORTRAN program itself. They require the help of JCL (Job Control Language). The JCL reserves many applicant solutions and finally selects the best solution among them.

7 Conclusion

The STP-CODE is a program developed by the authors, which is based on the classical steepest ascent method. Although the algorithm is a very old one, it can obtain the converged solutions automatically by introducing a lot of expertise based on our former experiences. Some examples of nonlinear optimal control problems in aerospace fields and their solutions are shown and explained. Some key technologies introduced into the program are briefly explained. The program is also useful to solve differential game problems, and an application is also shown, which would be difficult to solve by a current easy method on the market.

References:

[1] A. E. Bryson Jr. and W. E. Denham, A Steepest Ascent Method for Solving Optimum Programming Problems, *Journal of Applied Mechanics*, Vol.29, 1962, pp.247-257.

[2] A. K. Wu and A. Miele, Sequential Conjugate Gradient-Restoration Algorithm for Optimal Control Problems with Non-Differential Constraints and General Boundary Conditions, Part 1 , *Optimal Control Applications & Methods*, Vol.1, 1980, pp.69-88

[3] F. Imado, A Study on the Spacecraft Nonlinear Optimal Orbit Control with Low Thrusts, *Proc. of Second International Conference on Nonlinear Problems in Aviation and Aerospace* ,Vol.(1), 1998, pp.287-295.

[4] T.Fu and F. Imado, A Study about Optimal Trajectory Control of Dive and Ascent Satellite, *Proc. of the 2006 IEEE International Conference on Mechanics and Automation*

, 2006, pp.1008-1013.
[5] F. Imado and S. Miwa, Fighter Evasive Maneuver Against Proportional Navigation Missile, *AIAA Journal of Aircraft* , Vol.23, No.11,1986, pp.825-830
[6] T. Kuroda and F. Imado, Optimal Aircraft Maneuver Against Two Proportional Navigation Guided Missiles, *Proc. of 11th International Symposium on Dynamic Games and Applications*, 2006,CD-ROM.
[7] F. Imado and T. Kuroda, A Method to Solve Missile-Aircraft Pursuit-Evasion Differential Games, *Proc. of 16th IFAC World Congress*, 2005, CD-ROM
[8] F. Imado and T. Kuroda, A Solution of Missile-Aircraft Pursuit-Evasion Differential Games in Medium Range, *WSEAS Transaction on Systems*, Issue 2, Vol.6, 2006, pp.322-327
[9] F. Imado and A. Melikyan, The Development of the Solver for Nonlinear Optimal Control Problems in Aerospace Fields, *JSPS Report S05209*, 2006

Appendix

A steepest ascent method is a well-known algorithm to solve nonlinear optimal control problems. A summary of the algorithm is shown here for the readers' convenience.

Find $\bar{u}(t)$ to maximize (for minimizing, change the sign of the following ϕ)

$$J = \phi[\bar{x}(t_f)] \tag{A-1}$$

where

$$\dot{\bar{x}} = \bar{f}(\bar{x}, \bar{u}, t) \tag{A-2}$$

$$\bar{x}(t_0) = \bar{x}_0 \ : \text{specified} \tag{A-3}$$

with terminal constraints

$$\bar{\psi}[\bar{x}(t_f), t_f] = 0 \tag{A-4}$$

where $\bar{x}(t)$ is an n-dimensional state vector, $\bar{u}(t)$ is an m-dimensional control vector, and $\bar{\psi}$ is a q-dimensional constraint vector. The terminal time t_f is determined from the following stopping condition:

$$\Omega[\bar{x}(t_f), t_f] = 0 \tag{A-5}$$

The optimal control $\bar{u}(t)$ is obtained by the following algorithm.

1) Estimate a set of control variable histories $\bar{u}(t)$ (which is called a nominal control)
2) Integrate the system equations (A-2) with the initial condition (A-3) and control variable histories from step 1 until (A-5) is satisfied. Record $\bar{x}(t)$, $\bar{u}(t)$, and $\bar{\psi}[\bar{x}(t_f)]$. Calculate the time histories of the $(n \times n)$ and $(n \times m)$ matrices of functions:

$$F(t) = \frac{\partial \bar{f}}{\partial \bar{x}} \quad G(t) = \frac{\partial \bar{f}}{\partial \bar{u}} \tag{A-6}$$

3) Determine n-vector influence functions $\bar{\lambda}_\phi(t)$, $\bar{\lambda}_\Omega(t)$ and $(n \times q)$ matrix of influence functions $\lambda_\psi(t)$, by backward integration of the following influence equations, using $\bar{x}(t_f)$ obtained in Step 2 to determine the boundary conditions:

$$\dot{\bar{\lambda}}_\phi{}^T = -\bar{\lambda}_\phi \frac{\partial \bar{f}}{\partial \bar{x}} \tag{A-7}$$

$$\bar{\lambda}_\phi{}^T(t_f) = \left(\frac{\partial \phi}{\partial \bar{x}}\right)_{tf} \tag{A-8}$$

$$\dot{\bar{\lambda}}_\Omega{}^T = -\bar{\lambda}_\Omega \frac{\partial \bar{f}}{\partial \bar{x}} \tag{A-9}$$

$$\bar{\lambda}_\Omega{}^T(t_f) = \left(\frac{\partial \Omega}{\partial \bar{x}}\right)_{tf} \tag{A-10}$$

$$\dot{\lambda}_\psi{}^T = -\lambda_\psi{}^T \frac{\partial \bar{f}}{\partial \bar{x}} \tag{A-11}$$

$$\lambda_\psi{}^T(t_f) = \left(\frac{\partial \bar{\psi}}{\partial \bar{x}}\right)_{tf} \tag{A-12}$$

Calculate the following influence functions

$$\bar{\lambda}_{\phi\Omega} = \bar{\lambda}_\phi - \frac{\dot{\phi}(t_f)}{\dot{\Omega}(t_f)} \bar{\lambda}_\Omega \tag{A-13}$$

$$\lambda_{\psi\Omega} = \lambda_\psi - \frac{\dot{\bar{\psi}}(t_f)}{\dot{\Omega}(t_f)} \lambda_\psi \tag{A-14}$$

4) Simultaneously with Step 3 ,compute the following integrals:

$$I_{\psi\psi} = \int_{t0}^{tf} \lambda^T{}_{\psi\Omega} G W^{-1} G^T \lambda_{\psi\Omega} dt \tag{A-15}$$

$$\bar{I}_{\psi\phi} = \int_{t0}^{tf} \lambda^T{}_{\psi\Omega} G W^{-1} G^T \bar{\lambda}_{\phi\Omega} dt \tag{A-16}$$

$$I_{\phi\phi} = \int_{t0}^{tf} \bar{\lambda}^T{}_{\phi\Omega} G W^{-1} G^T \bar{\lambda}_{\phi\Omega} dt \tag{A-17}$$

5) Choose values of $\delta\bar{\psi}$ to cause the next solution to be closer to the desired values $\bar{\psi}[\bar{x}(t_f)] = 0$. For example, one might choose

$$\delta\bar{\psi} = -\varepsilon\bar{\psi}[\bar{x}(t_f)], \quad 0 < \varepsilon \le 1 \tag{A-18}$$

The proper choice of $\delta\bar{u}(t)$, which increases the performance index J is given as follows:

$$\delta\bar{u}(t) = (1/2\mu) W^{-1} G^T (\bar{\lambda}_{\phi\Omega} - \lambda_{\psi\Omega}\bar{v}) \tag{A-19}$$

where

$$2\mu = \left[\frac{I_{\phi\phi} - \bar{I}_{\psi\phi}{}^T I_{\psi\psi}{}^{-1} \bar{I}_{\psi\phi}}{(dp)^2 - d\bar{\psi}^T I_{\psi\psi}{}^{-1} d\bar{\psi}}\right]^{\frac{1}{2}} \tag{A-20}$$

$$\bar{v} = -2\mu I_{\psi\psi}{}^{-1} d\bar{\psi} + I_{\psi\psi}{}^{-1} \bar{I}_{\psi\phi} \tag{A-21}$$

where dp and $(m \times m)$ matrix of weighting functions $W(t)$ are chosen to satisfy

$$(dp)^2 = \int_{t0}^{tf} \delta\bar{u}^T(t) W(t) \delta\bar{u}(t) dt \tag{A-22}$$

6) Repeat Steps 1-5, using an improved estimate of $\bar{u}(t)$ where

$$\bar{u}(t) = \bar{u}(t)_{old} + \delta\bar{u}(t) \tag{A-23}$$